minerals

MDPI

Article

Characterization and Economic Potential of Historic Tailings from Gravity Separation: Implications from a Mine Waste Dump (Pb-Ag) in the Harz Mountains Mining District, Germany

Kerstin Kuhn * and Jeannet A. Meima

Federal Institute for Geosciences and Natural Resources (BGR), Stilleweg 2, 30655 Hannover, Germany; jeannet.meima@bgr.de

* Correspondence: kerstin.kuhn@bgr.de; Tel.: +49-(0)511-643-3370

Received: 4 April 2019; Accepted: 14 May 2019; Published: 16 May 2019

Abstract: In contrast to modern tailings from froth flotation, little is known about historic tailings from gravity separation. However, they may be of economic interest due to their higher metal grades compared to modern tailings. As an example for these types of historic tailings, the inner structure, as well as the economic potential (Pb, Zn, Cu, Ag, Sb), of the old Bergwerkswohlfahrt mine waste dump in Germany were studied. The investigations focused on textural, geochemical, and mineralogical properties. For this purpose, an extensive drilling program was undertaken. The drill cores were subsequently analyzed with a laser-induced breakdown spectroscopy (LIBS) core scanner to obtain the detailed spatial distribution of potentially valuable elements. The fine-sized residues could be differentiated into different layers, all of them including valuable metals in varying proportions. The strong variations in stratification and in metal distribution over short distances are caused by the batch-wise deposition of the tailings. This heterogeneity within short distances has to be taken into account for future exploration of these types of deposits. The application of a core scanner using LIBS is very convenient for detailed spatial analysis of drill cores, however, the calibration effort, particularly for heterogeneous sample material, is proportionally large. The valuable metal content for Bergwerkswohlfahrt was estimated to be 8000 metric tons of Pb and 610,000 ounces of Ag. Although of limited economic value, recycling might finance future remediation costs. Furthermore, the occurrence of historic tailings in nearby clusters may present further recycling opportunities.

Keywords: mine waste; tailings; gravity separation; stamp mill; historic tailings; metals; exploration; economic potential; LIBS; core scanner

1. Introduction

Mine waste may not only pose an environmental risk [1–6], but may also represent potential sources of valuable minerals and metals. However, the latter holds true less for waste from current mining activities, as this is defined as "those waste products originating, accumulating, and present at mine sites, which are unwanted and have no current economic value" [4]. However, economic potential can be attributed much more to historic mine waste products and especially to those originating from ore extraction, because modern extraction technologies are more efficient compared to earlier technologies. Depending on its origin, three types of mine waste can be differentiated, namely, mining waste (e.g., non-mineralized and low-grade mineralized waste rocks), processing waste (e.g., tailings), and metallurgical waste (e.g., slags, flue ashes, dusts, bauxite red mud, or phosphogypsum).

Current re-use and recycling of mine waste, especially tailings, include its use as backfill, production of bricks, and extraction of minerals and metals. However, compared to primary deposits,

in many younger tailings from froth flotation, metal contents are relatively low. In general, average base metal contents given in the literature are below 2.4 wt % Zn, 1.2 wt % Pb, 0.4 wt % Sn, and 0.2 wt % Cu, respectively, and in most cases even below 1 wt % Zn and 1 wt % Pb [7–11].

According to Gordon [12], concentrations of Cu in North American copper ore tailings were 0.75 wt % when froth flotation was introduced to mining after 1900. Until the end of the 20th century, Cu concentrations decreased continuously down to 0.09 wt %. Of course, this decrease was also an effect of mining of ores with lower Cu grade.

As base metal contents in modern tailings are low and recycling of the mostly fine-grained material is challenging, in general the more expensive metals, above all Au, are recycled. However, there are also other examples, such as the recycling of Co by bioleaching of pyrite rich tailings (concentrate stockpiles) of the Kilembe Cu-mine, Uganda [13], and the extraction of Cu and Mo from the Colihues tailings pond in combination with fresh tailings from the Cu mine in El Teniente, Chile [14].

In contrast, little is known about older tailings, as before the introduction of froth flotation into mining, ore processing methods were much simpler (e.g., by stamp mills in combination with gravity separation), thus metal concentrations in old tailings are generally higher.

In literature, little information is available about the economic potential of these types of tailings. Neither have the old tailings been investigated in enough detail, and if only for ecological reasons [15–17], nor is there a precise differentiation between tailings and mine waste of the various other types. As mentioned above, metal contents of historic tailings based on gravity separation compared to modern tailings based on froth flotation are generally much higher.

Examples are:

- 10 wt % Pb, and even up to 15 wt % Pb in tailings of the Whitespots lead mines (19th century) near Newtownards, Northern Ireland [15].
- 9.6 and 16.6 wt % Pb in two composite samples of tailings of the Pontigbaud lead-silver mine, France [17]. From the same mining district Bellenfant et al. [16] reported concentrations of 0.6–7 wt % Pb in historic tailings.
- Surface samples of 20 piled-up tailings in the Sierra Mineral of Cartagena-La Unión mining district, Spain, showed concentrations of 4–5.4 wt % Zn, 0.5–3.2 wt % Pb, and 233–645 ppm Cu [18].
- Nine samples of stamp mill tailings from the La Quintera and Promontoria silver mines, Alamos mining district, Mexico, still contained 100 ppm Ag and 0.1–0.3 ppm Au [19].
- Cu in tailings from US copper mining before 1900, i.e., before introduction of froth flotation, were above 0.9 wt % [12].

Besides the data given above, not much is known about the characteristics of these old tailings. Representative for many of them is the old Bergwerkswohlfahrt mine waste dump in Germany. In this paper, the economic potential of this typical old tailings dump has been investigated on the basis of intense sampling campaigns. This is also the first publication giving details about the internal structure and the metal distribution of such a secondary deposit.

Exploration of the mine waste dump was done by direct push drilling with extensive core sampling. In order to obtain a detailed spatial distribution of potentially valuable elements (Pb, Zn, Cu, Ag, Sb), most of the drill cores were subsequently analyzed with a core scanner based on laser-induced breakdown spectroscopy (LIBS). This analytical method was already proven to work successfully in tailings by Khajehzadeh et al. [20] and Kuhn et al. [21]. LIBS was used to possibly reduce costs and to analyze larger amounts of cores within a shorter time. Additional mineralogical and geochemical analyses were performed on selected samples for reference purposes.

2. Materials and Methods

2.1. Study Area

The investigated mine waste dump "Bergwerkswohlfahrt" is situated between the former mining towns of Clausthal-Zellerfeld and Bad Grund in the historic Harz Mountains mining district in central Germany. In this district hydrothermal veins enriched in base metals were mined between the Middle Ages and 1992 [22,23]. The mine waste dump is mainly built up of tailings of a stamp mill of the historic "Bergwerkswohlfahrt" silver and lead mine.

Between 1822 and the 1950s, lead- and silver- rich hydrothermal veins from the eastern part of the "Silbernaaler" vein system were mined in the Bergwerkswohlfahrt underground mine [22,23]. After barite became a raw material of commercial interest, it also was occasionally produced in the 19th and 20th century [22]. In 1923, the two nearby mines Bergwerkswohlfahrt and Hilfe Gottes, which were already connected below the surface, were merged into the "Erzbergwerk Grund" [22]. As the highest silver concentrations were restricted to the upper parts of the vein, which were mined out in the Middle Ages, mining shifted to silver-containing galena after 1590 [22].

The focus of this study are the tailings of the Bergwerkswohlfahrt mine waste dump (Figure 1), which were deposited between 1903 and 1931 [24]. From 1595 until the introduction of froth flotation in the 1930s, water-powered stamp mills were used in the beneficiation processes at many mine sites in the Harz Mountains [22]. A stamp mill is a machine that crushes material by pounding rather than by grinding. The crushed ore was treated mainly by jigging or on shaking tables in order to concentrate the valuable heavy minerals.

Between 1903 and 1914, as much as 25,000–30,000 tons of crude ore was processed per year [22]. Since 1916, up to 40,500 tons of ore could have be mined [22]. Due to the global economic crisis, the ore processing plant of Bergwerkswohlfahrt was closed in 1931. From that time on, until ore resources of the Bergwerkswohlfahrt mine were exhausted during the 1950s, the mined ore of Bergwerkswohlfahrt was transported underground to the Hilfe Gottes mine and processed there [22,23].

Nowadays, the Bergwerkswohlfahrt mine waste dump is about 400 m long and is wedge-shaped. It is a sidehill fill [25] constructed on sloping terrain and is located adjacent to the "Innerste" stream (Figure 1). Due to the high heavy metal concentrations of the tailings, they are hardly covered by vegetation. Only in some areas can a sparse vegetation of grass or small trees be observed. Due to this lack of vegetation, combined with the steep slopes, there is an input of mineralized residue into the adjacent "Innerste" stream. For this reason, remediation of this dump is a high priority.

Figure 1. Location of the Harz Mountains in Germany (red circle; [26]) and photo of the northwestern part of the Bergwerkswohlfahrt mine waste dump (source: Federal Institute for Geosciences and Natural Resources (BGR)). The image width is approximately 150 m.

The Bergwerkswohlfahrt mine waste dump is quite heterogeneous and consists of large areas with stamp mill tailings alternating with areas consisting of blocky material (Figure 2). The tailings consist of a mixture of sand- to silt-sized material, with some gravel-sized rock fragments. The latter is made up of gangue and ore minerals, as well as country rock, which are partially intergrown.

The blocky material consists of rock fragments mixed with loam. Poggendorf et al. [27] mentioned a partial removal of the ore processing residues and its use as aggregates, as well as the use of the dump as a landfill site for excavated soil. The precise location of the excavated soil has not been documented. However, most probably the blocky material under tree cover represents this excavated soil. Additionally, slags were found adjacent to the dump (Figure 2).

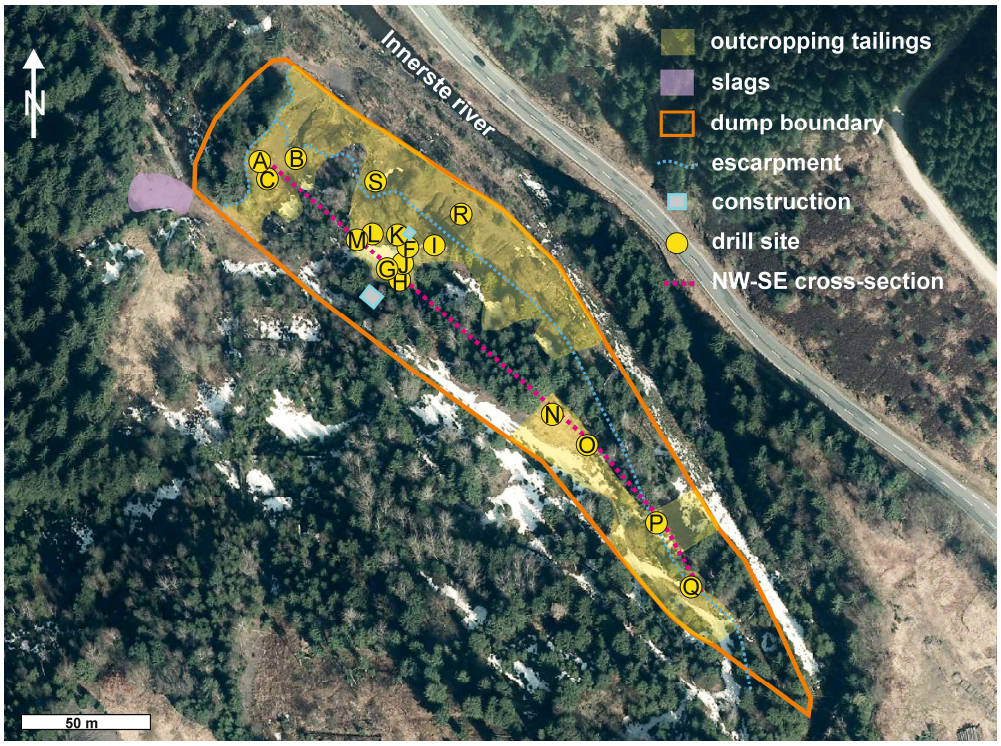

Figure 2. Aerial photo [28] of the Bergwerkswohlfahrt mine waste dump showing its boundary [29], as well as the drilling locations. The surface outcrops of the tailings are shown in transparent yellow.

2.2. Drilling and Sample Handling

The applied drilling method was direct push core drilling. The cores were collected in plastic liners. In total, 16 cores were collected as part of three drilling campaigns (Figure 2). In the center of the mine waste dump more cores were drilled compared to its peripheral areas in order to better evaluate the spatial variability of the metals of economic interest. The location of the central drill holes were predetermined by a geophysical campaign, which was part of a joint research project on this mine waste dump [30–32].

Due to the small diameter of the drill pipe (5 cm) and the included plastic liners, drilling into the coarse-grained blocky material covering parts of the dump was not possible. Therefore, only areas with ore processing residues at the surface were sampled by drilling. The drill pipes could be rammed down to 4–8 m depth, where most of them got stuck in rocky material. This rocky material represents the underlying bed, which is made up of fragments of country rock, partly intergrown with gangue and ore minerals. This bed seems to be mining waste, which may be derived from the construction of the adits, shafts, and surface infrastructure in former times.

Because direct push drilling does not allow for casing of the drill hole, some loose material fell into the drill hole during the time that the drill pipes were outside the hole to extend their length. This caving material was documented and was not included in the data below.

Cores A and B were part of the first drilling campaign. Both cores were cut in half and air-dried. Afterwards, they were sampled in detail according to the observed changes in texture and color. In total, 102 individual samples were taken from cores A and B, covering the complete length of both cores. The samples were then subjected to bulk chemical analyses with X-ray fluorescence (XRF) and acid digestion/inductively coupled plasma-atomic emission spectroscopy (ICP-OES), as described in Section 2.3.2.

Core C was part of the second drilling campaign. Core C had no plastic liner and was completely sampled (n = 30) in the field according to the observed changes in texture and color. Bulk chemical analyses were carried out with XRF and laser ablation-inductively coupled plasma-mass spectrometry (LA-ICP-MS).

Fourteen additional cores (F–S) were taken in a third drilling campaign. The cores were cut in half, air-dried, and subjected to LIBS core scanning, as described in Section 2.3.1. After core scanning, representative core sections were sampled in order to obtain reference samples for subsequent LIBS calibration. Multivariate LIBS calibration requires reference samples that are representative for the observed differences in chemical and mineralogical composition. Therefore, three cores (K, R, Q) with different stratigraphy were sampled in detail for the complete core length. For each stratigraphic layer, one sample was taken (n = 121). Additional stratigraphic layers were sampled from the remaining cores (F, S, I, L, O, G, M, H; n = 23). These layers include similar stratigraphic layers from spatially different areas of the dump, as well as stratigraphic layers, which do not occur in the three completely sampled cores. The size of the samples varies between 1 and 50 cm in length (mean 10 cm), 5 cm in width, and about 1.5–2 cm in depth, and comprise tailings as well as underlying blocky material. The reference samples were analyzed with XRF and LA-ICP-MS, as described in Section 2.3.2.

2.3. Methods

2.3.1. LIBS Core Scanning and PLS Regression Method

Element mapping of the drill core sections was performed using a LIBS core scanner manufactured by LTB–Lasertechnik Berlin. LIBS is an atomic emission spectroscopy method. For excitation, a very short duration laser pulse is used to generate a plasma on the sample surface and to vaporize a small amount of sample material. As the plasma expands and cools the atoms and molecules emit light at their characteristic wavelengths. Therefore, the obtained emission spectrum is characteristic for the elemental composition of the sample. Further information about this method can be found in Body and Chadwick [33], Cremers and Radziemski [34], and Miziolek et al. [35].

The specifications of the used core scanner are summarized in Table 1 and the operating principle is described in Kuhn et al. [21]. Each core meter was mapped, with a step size of 0.5 mm along the core and a step size of 2 mm over 20 mm across the core. This resulted in 20,000 spectra per core meter. At each measurement point, five laser shots were fired and the collected light was accumulated into one spectrum [21]. Measurements were run directly on the dried core surface under ambient atmosphere and atmospheric pressure. An exhaust system close to the sample surface prevented the production of dust clouds.

From each spectrum, the spectral intensities of several characteristic emission lines of main, minor, and trace elements were calculated as peak area integrals, with a peak width of 0.05 nm [21]. Further data processing included normalization of each wavelength channel to the integrated total energy of that spectrum.

For quantification of the LIBS intensities from heterogeneous material, an extensive calibration by means of multivariate calibration approaches is required. The authors selected the partial least square regression (PLS or PLSR), which has often successfully been used for LIBS calibration [36–39].

The possibility of the application of PLS for LIBS measurements of tailings from froth flotation was shown by Khajehzadeh et al. [20] and Kuhn et al. [21]. The PLS algorithm can cope with numerous X-variables, which are often correlated and simultaneously model several response Y-variables [40]. Detailed information of the PLS regression and its applications are given in Geladi and Kowalski [41], Höskuldsson [42], Naes and Martens [43], Sirven [36], Wold et al. [40,44], and Yaroshchyk et al. [37].

Table 1. Specifications of the applied laser-induced breakdown spectroscopy (LIBS) core scanner.

Laser	**Q-Switched Neodymium-Doped Yttrium Aluminum Garnet Solid-State Laser (Nd:YAG)**
Wavelength	1064 nm
Pulse width	11 ns
Energy	55 mJ/pulse
Repetition rate	20 Hz
Spot size	200 µm
Spectrometer	**Echelle Spectrometer**
Spectral range	285–964 nm
Spectral resolution	R = 10,000 (resolution: 0.29–0.96 nm)
Detector	**Charge-Coupled Device (CCD)**
Resolution	1024 × 256 pixel
Delay time	1.5 µs

The development of the PLS calibration models for cores F–S was based on the 144 different material-specific reference samples (training set: 92 calibration samples; test set: 52 validation samples) that were obtained from relatively homogenous core sections, as described in Section 2.2. Median LIBS intensities were calculated for the regions representing the location of the reference samples. Metals that show a strong geochemical correlation, e.g., Pb, Ag, and Sb, were calibrated together in the same PLS model. Additional PLS calibration models were developed for Cu and Zn, respectively. The R-package "pls" [45] was used for PLS analysis. The number of latent variables, as well as further benchmarks for the prediction performance of the used PLS models, are given in Table 2. The PLS model was run with scaling on, which explains why only 3–5 latent variables (components) were necessary to establish suitable PLS models. Scaling here means that each variable was standardized by dividing each variable value by its standard deviation.

Table 2. The prediction performance of the partial least square regression (PLS) models for LIBS core scanner data. The limit of detection (LOD), the coefficient of multiple correlation R^2, as well as the root mean square error of prediction (RMSEP) refer to the test set (52 validation samples), which was used for model validation.

Element	**Unit**	**Calibration of PLS Model (92 Samples)**		**Validation of PLS Model (52 Samples)**	
		Concentration Range of Model	**Latent Variables**	**RMSEP**	R^2
Pb	wt %	0–10	3	1.4	0.74
Zn	ppm	0–2500	3	330	0.67
Cu	ppm	0–800	5	110	0.55
Ag	ppm	0–250	3	40	0.73
Sb	ppm	0–550	3	80	0.71

A comparison of the bulk chemical concentrations of the reference samples with the predicted LIBS concentrations shows good correlation, despite possible 2D and 3D artefacts in the reference samples (Figure 3). Possible 2D and 3D artefacts may arise when the surface of the drill core that is

measured with LIBS is significantly different in composition from the bulk 3D material, which was sampled for bulk chemical analysis. Of course, the size of the reference samples was chosen to be large enough to minimize such effects.

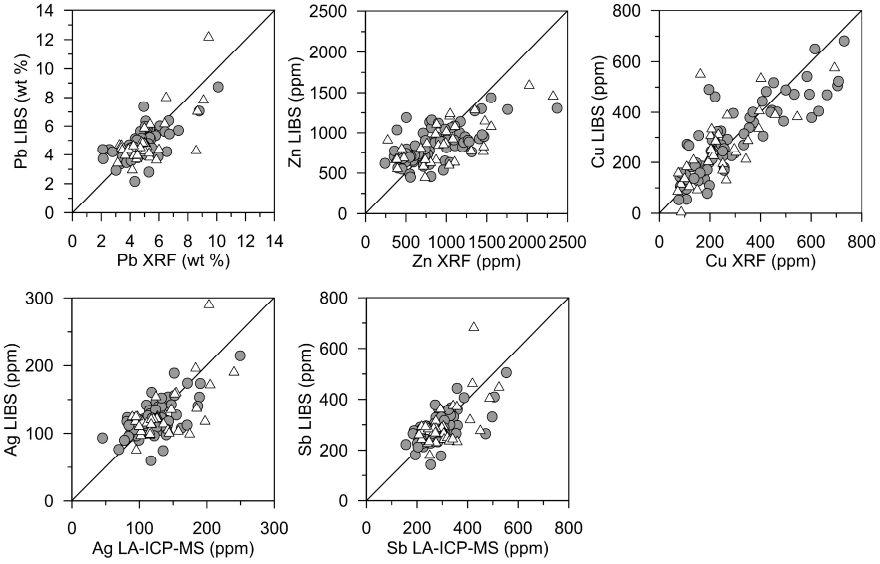

Figure 3. Comparison of predicted concentrations obtained by laser-induced breakdown spectroscopy (LIBS) + partial least square regression (PLS) versus reference concentrations obtained by X-ray fluorescence (XRF) or laser ablation-inductively coupled plasma-mass spectrometry (LA-ICP-MS) for the reference tailing samples. The training set for the PLS model is represented by closed circles, and the open triangles represent the test set.

Regarding the valuable metals Pb, Zn, Cu, Ag, and Sb investigated in this study, the predictive plots show a distinct linear correlation between the LIBS-area-based concentrations and the bulk chemical concentrations. The PLS models are valid for the concentration ranges shown in Table 2. The model is not configured for a strong extrapolation beyond these limits.

The reference samples were selected in accordance with the existing concentration ranges for the investigated cores. Close examination of the concentration ranges of the PLS model has confirmed that the PLS model is indeed consistent with the observed variations in LIBS intensities and bulk element concentrations in each of the drilling cores.

To determine the spatial distribution of the valuable metals within the drill cores of the mine waste dump, the PLS calibration model was applied on average LIBS spectra for core intervals of 20 mm width × 50 mm length. Thereby, up to 1000 single spectra result in average metal concentrations of core intervals of 50 mm length. Averaging is necessary to ensure that the resulting LIBS spectra are within the range of the PLS calibration model. Very high and very low metal concentrations originate in the high spatial resolution of the LIBS method, e.g., when the 200 µm wide LIBS-Laser hits larger and almost pure quartz or sulfide particles. Caved material was skipped for each core meter.

2.3.2. Bulk Chemical Analyses

Concentrations of major and minor elements of all reference samples were obtained by wavelength dispersive X-ray fluorescence (XRF). Analyses were performed by means of two wavelength dispersive sequential spectrometers (AXIOS and PW2400, PANalytical, Almelo, The Netherlands) with a Rh and Cr tube, respectively. Measurements were done on fused glass discs, which were produced from the annealed sample powders in combination with lithium metaborate and a lithium bromide solution.

Determination of concentrations of trace elements was done by laser ablation-inductively coupled plasma-mass spectrometry (LA-ICP-MS). For LA-ICP-MS analyses an "Element XR ICP-MS" (Thermo Fisher Scientific, Bremen, Germany) was used in combination with a 193 nm laser ablation system (New

Wave UP193-FX, Elemental Scientific Lasers, Bozeman, MT, USA). Analyses were performed on pressed pellets from pure sample powders, which were ground to analytical fineness. NIST 612 (National Institute of Standards and Technology, Gaithersburg, MD, USA) was used as calibration material. The SiO_2-content (XRF measurements) of each sample was used as an internal standard. The quality of the obtained data was check by multiple analysis of the commercially available reference materials CGL108 (Central Geological Laboratory, Ulaanbaatar, Mongolia), NCSDC29105, and NCSDC73508 (China National Analysis Center for Iron and Steel, Beijing, China). The obtained mean values are in agreement with the certified values within a range of ±10%.

For analysis of Ag in core A and B, HNO_3 digestion (EPA Method 3051A) was applied for all samples followed by inductively coupled plasma-atomic emission spectroscopy (ICP-OES) analysis. The HORIBA Jobin Yvon spectrometer used (model JY 166 ULTRACE, Bensheim, Germany) was calibrated with commercial multi-element standard solutions. Detection limit and accuracy were 1.2 ppm and 5%, respectively.

2.3.3. Mineralogical Analyses

For characterization of the different tailing layers, qualitative mineralogical analyses were examined by X-ray diffraction (XRD; PANalytical X'Pert PRO MPD Θ-Θ diffractometer, Almelo, The Netherlands) of 97 powder samples. The samples were derived from seven drill cores (A, B, K, R, Q, F, O) covering all areas of the dump and all different types of ore processing residues.

Detailed mineralogical investigations of the valuable metal bearing phases and weathering processes within the tailings were done by transmitted light and reflected light microscopy, as well as by scanning electron microscopy (Quanta 650F, FEI/Thermo Fisher Scientific, Eindhoven, The Netherlands). A total of 42 polished thin sections were examined.

2.3.4. Grain Size Analyses

Grain size analyses were conducted for 29 samples from different types of ore processing residues (from drill cores K, R, Q, F, S). Each drill hole was sampled for all types of residual material, which were optically distinguishable as fine-grained, medium-grained, and coarse-grained layers. Only homogeneous layers of sufficient thickness were sampled to obtain enough material for particle size analyzes. Grain sizes were measured by dry sieving, and for grain sizes <63 µm by a SediGraph (Micromeritics, Norcross, GA, USA). Dry sieving was done using standard 200 mm analytical sieves of 63 µm, 112 µm, 200 µm, 355 µm, 630 µm, 1.12 mm, and 2 mm mesh size. An agglomeration of fine particles could not be observed during sieving.

3. Results and Discussion

3.1. Mineralogy of the Mine Waste Dump

Compared to other mine waste dumps in the Harz Mountains [46], the residues of the Bergwerkswohlfahrt mine waste dump contain high concentrations of lead, silver, and antimony. Based on bulk chemical analysis, concentrations are between 2.1–14.4 wt % Pb, 3–268 ppm Ag, and 46–642 ppm Sb. Since a mainly lead-rich ore was mined in this area of the Silbernaaler vein system, the zinc and copper concentrations of the residues are accordingly low. They are between 240–6284 ppm Zn and 69–2249 ppm Cu.

Mineralogical analyses of the tailings revealed a composition of mainly quartz (SiO_2) and muscovite ($KAl_2(AlSi_3)O_{10}(OH)_2$). Further minerals in minor amounts include barite ($BaSO_4$), various carbonates, such as siderite ($FeCO_3$, which can also contain some Mg), ferroan dolomite ($Ca(Mg,Fe)(CO_3)_2$,), ankerite ($Ca(Fe,Mg,Mn)(CO_3)_2$), and small amounts of calcite ($CaCO_3$), as well as orthoclase ($KAlSi_3O_8$) and albite ($NaAlSiO_3O_8$). Most of the quartz, barite, and the carbonates originated from gangue minerals of the mined hydrothermal veins. The rest of the quartz, as well as muscovite and feldspar, can be traced back to fragments from the wall rocks (greywacke and slate).

The primary sulfidic ore minerals within the tailings are galena (PbS), followed by minor amounts of sphalerite ((Zn,Fe)S), pyrite (FeS_2), chalcopyrite ($CuFeS_2$), silver-bearing tetrahedrite ($(Cu,Ag)_{10}(Zn,Fe)_2Sb_4S_{13}$), freibergite ($(Ag,Cu)_{10}(Zn,Fe)_2Sb_4S_{13}$), and bournonite ($PbCuSbS_3$). Stephanite ($Ag_5SbS_4$) was observed as an accessory mineral. Figure 4 shows images of the main sulfides.

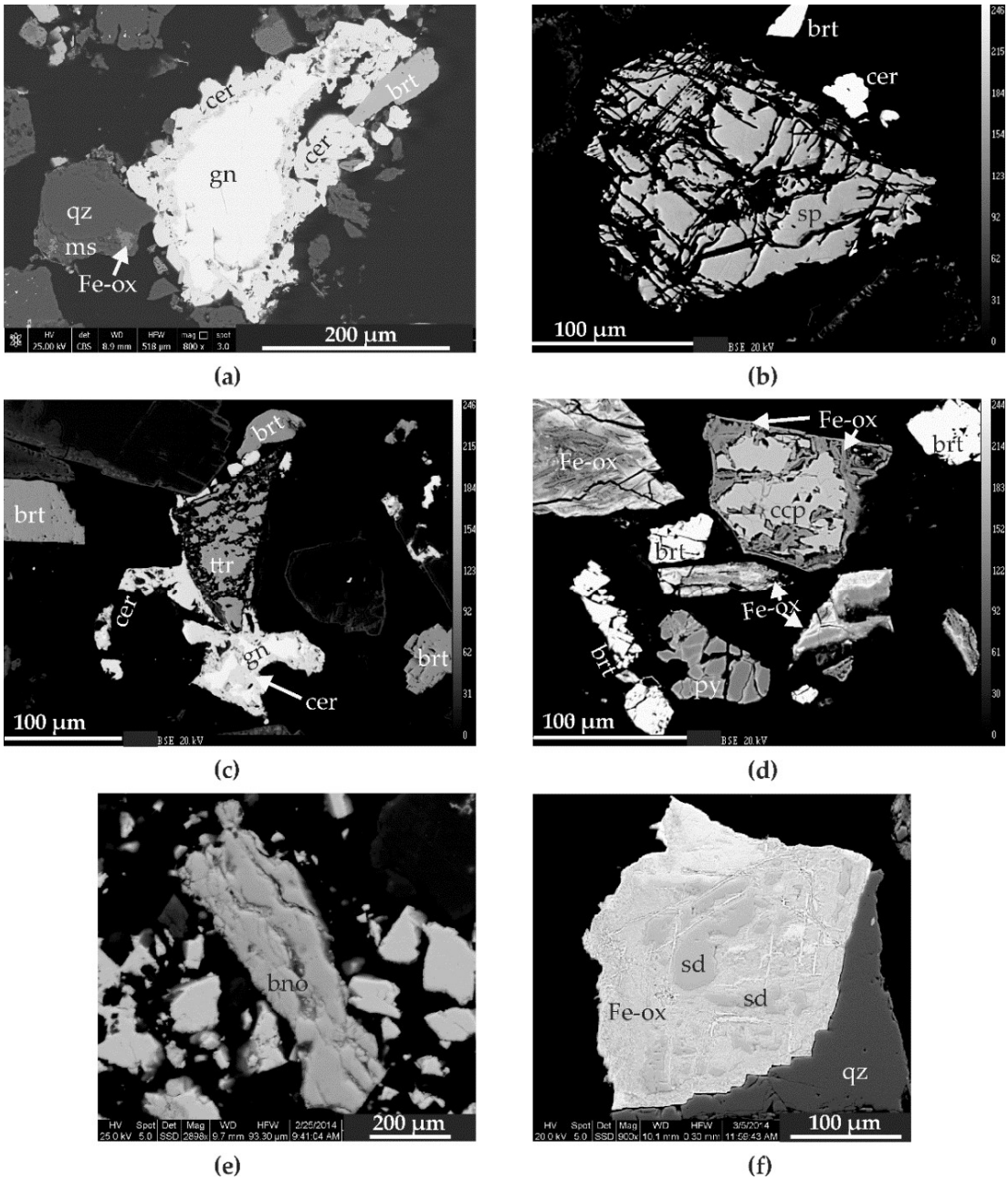

Figure 4. Backscattered-electron images of tailings, showing: (**a**) alteration of galena (gn) to cerussite (cer); (**b**) sphalerite in a state of partial dissolution; (**c**) corroded Ag-rich tetrahedrite (ttr) and galena (gn) partially weathered to cerussite (cer); (**d**) different forms of weathering with fractured pyrite (py) and chalcopyrite (ccp) being weathered to Fe oxyhydroxides at the rim and along cracks; (**e**) corroded bournonite (bno); (**f**) advanced weathering of siderite to Fe oxyhydroxides (Fe-ox) with siderite (sd) remaining in the core area. The lighter the Fe oxyhydroxides, the more Mn, Pb, and other metals they contain in general. Note: qz—quartz, ms—muscovite, brt—barite, Fe-ox—Fe oxyhydroxides, cer—cerussite.

Secondary minerals and phases formed by weathering in the mine waste environment include cerussite ($PbCO_3$), Fe oxyhydroxides, and in some layers secondary gypsum ($Ca(SO_4)_2{\cdot}2(H_2O)$) and calcite. In some cases, calcite is cementing other grains. In minor amounts, framboidal pyrite occurs. Smithsonite ($ZnCO_3$) and secondary silver phases, with the latter being unstable in the SEM or microprobe beam, were found as accessory minerals. Large galena grains that were not encapsulated in larger particles were observed with a cerussite alteration rim (Figure 4), which presumably protects the remaining galena. Small galena grains, however, are completely weathered to cerussite. Weathering processes were probably favored by the high content of Ag, Sb, and partially Cu in the galena [47,48], which occur in the form of Sb-Ag-rich- or subordinate Sb-Cu-rich exsolutions.

As oxidizing conditions prevail in most parts of the mine waste dump, all primary sulfides show signs of weathering unless they are encapsulated in other minerals. Most sulfides show corroded margins, cracks, or holes (Figure 4). Secondary Fe oxyhydroxides replacing the sulfides rarely occur. Only chalcopyrite is clearly weathered to Fe oxyhydroxides at its margins and along cracks (Figure 4).

Relatively large metal(loid)-rich Fe-oxyhydroxide grains were commonly observed as weathering products after siderite. The Fe oxyhydroxides inherit the grain shapes of the siderite grains and can contain remains of them (Figure 4). As this displacement can be observed in various stages of development, the siderite nuclei cannot be interpreted as inclusions in less stable carbonates or newly formed secondary siderites, which have been described in a few tailings [49,50].

Metals released by weathering can be adsorbed or co-precipitated with the metal(loid)-rich Fe oxyhydroxides [51]. In variable proportions, the Fe oxyhydroxides in the investigated mine waste dump contain large amounts of Pb and Mn, and occasionally also of Zn, Cu, Sb, Ag, and other trace elements. In contrast, traces of Ag were found in only a few cerussites, although the primary galena is rich in Ag and Sb.

The occurrence of cerussite as the weathering product of galena, as well as the lack of anglesite ($PbSO_4$), which is usually formed in acidic environments [47,52], indicates a pH neutral oxidizing environment. Common batch leaching tests, according to DIN 38414-4 (S4) [53], of near-surface tailing material of the Bergwerkswohlfahrt mine waste dump revealed a pH value of 7.4 [54]. For these reasons it can be assumed that since their deposition about 100 years ago, the neutralization potential of the dump has been high enough to prevent the formation of acid mine drainage. Carbonates play an important role in limiting acid rock drainage [51,52,55]. As only small amounts of calcite occur and many siderites are strongly weathered to Fe oxyhydroxides, siderite may be an important buffer mineral in this system. Ferroan dolomite and ankerite even seem to be more resistant than siderite under the prevailing conditions.

3.2. Types of Ore Processing Residues

The tailings of the investigated dump are characterized by three types of layers, which are distinguishable by their grain size: sand, silty sand, and clayey silt. However, they also intermix with each other and should, therefore, be understood as end members. Figure 5 shows the distribution of the three types of layers within the cores taken. It is clearly visible that the mine waste dump is quite heterogeneous. Especially in the northwestern area of dump site, layers of clayey silt of a few cm to 1 m thickness are common, which, on the other hand, are almost absent in the southeastern tail. Since the amount of silty sand layers in the southeastern area is also low, sand remains as the dominating grain size.

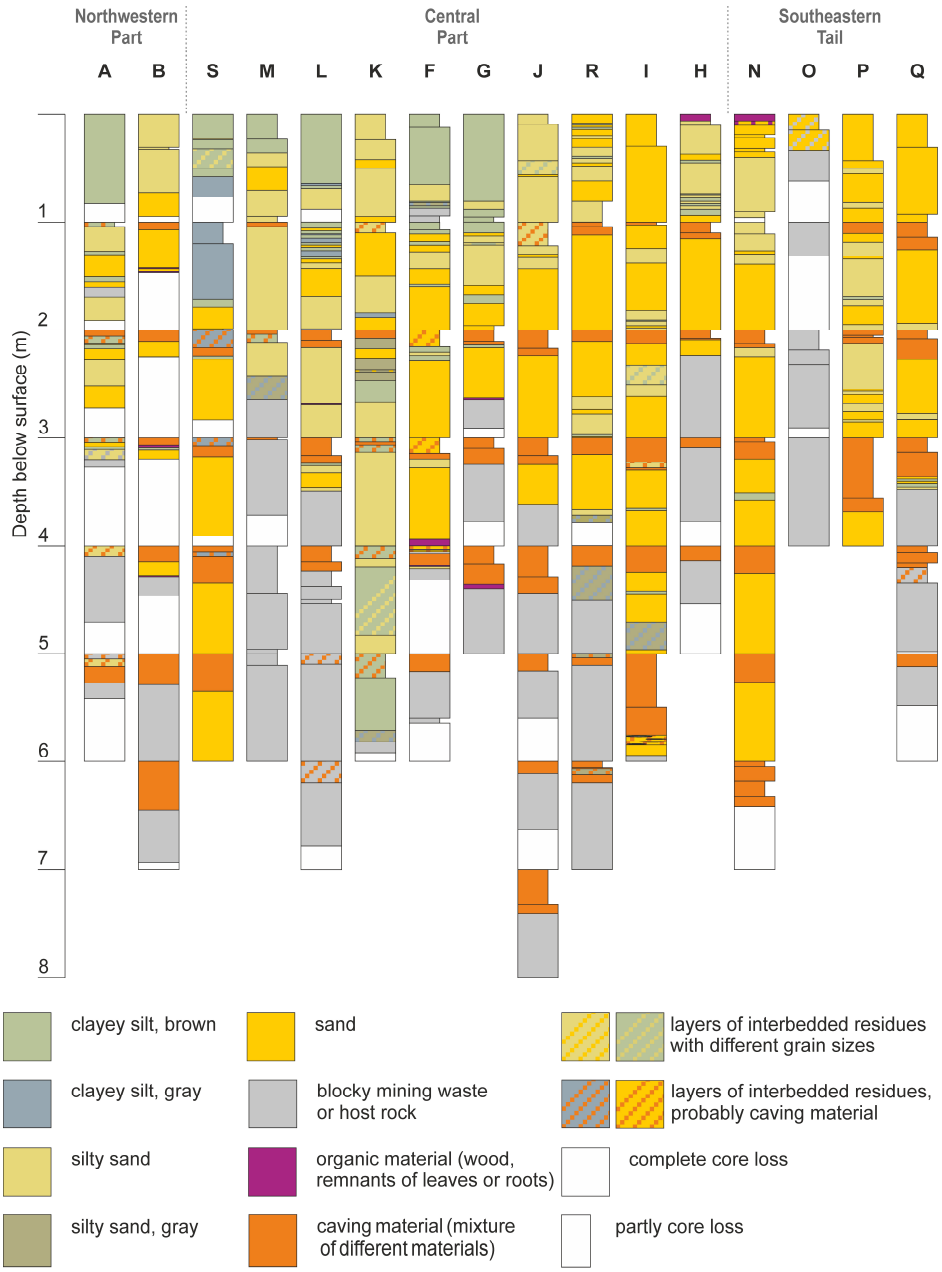

Figure 5. Lithology of cores taken in Bergwerkswohlfahrt mine waste dump, roughly sorted from northwest to southeast.

The various types of layers differ not only in grain size composition but also in their mineralogical and chemical composition (Table 3). Since the metal concentrations for the whole set of samples, as well as for samples from individual layer types, are not normally distributed, but are bimodal or strongly left-skewed or right-skewed, the median and the percentiles are used for characterization. One cause of the deviation from the normal distribution was the fluctuating composition of the mined crude ore, which was usually rich in Pb, Ag, and Sb but had very different Zn and Cu contents. The Zn and Cu distribution in the layers, therefore, deviates much more from the normal distribution than Pb, Ag, and Sb (see mean and median in Table 3). In addition, subsequent weathering processes within the dump change the metal distribution in the tailings.

Table 3. Statistics of the chemical composition of the tailings from the Bergwerkswohlfahrt mine waste dump. Only drill core samples are considered, which can be clearly assigned to one of the three layer types. Analyses are based on X-ray fluorescence (XRF), inductively coupled plasma-atomic emission spectroscopy ICP-OES, and laser ablation-inductively coupled plasma-mass spectrometry (LA-ICP-MS) analyses. Total iron is calculated as Fe_2O_3.

Statistics	Pb wt %	Zn ppm	Cu ppm	Ag ppm	Sb ppm	SiO_2 wt %	Fe_2O_3 wt %	Al_2O_3 wt %	K_2O wt %	CaO wt %	MgO wt %	MnO wt %	Ba wt %
Sand layers (n = 51)													
Min	2.1	240	69	45	116	56.7	5.1	5.4	1.2	0.1	0.2	0.6	0.4
Q_1	3.7	580	108	90	224	64.3	6.5	6.5	1.4	1.0	0.7	0.8	0.8
Median	**4.2**	**855**	**162**	**106**	**248**	**66.7**	**7.8**	**6.8**	**1.5**	**1.3**	**0.9**	**1.1**	**1.3**
Mean	4.2	1160	253	108	258	65.9	8.0	6.7	1.5	1.2	0.8	1.1	1.3
Q_3	4.8	1460	256	126	310	68.2	8.8	7.2	1.6	1.6	1.0	1.3	1.7
Max	6.4	6200	2250	174	412	70.5	15.0	8.0	1.8	2.3	1.2	2.6	4.0
Silty sand layers (n = 50)													
Min	0.3	644	104	3	46	8.0	6.7	0.5	0.1	0.1	0.2	0.9	0.3
Q_1	3.4	740	195	79	232	52.1	7.7	3.8	0.8	0.2	0.3	1.1	1.9
Median	**5.0**	**1340**	**331**	**125**	**306**	**58.4**	**11.0**	**6.1**	**1.3**	**0.7**	**0.6**	**1.6**	**4.5**
Mean	4.8	1890	389	124	303	53.9	11.9	5.9	1.3	1.0	0.6	1.8	5.6
Q_3	5.8	3440	695	173	378	60.8	18.4	7.2	1.6	1.7	0.9	3.2	8.9
Max	7.4	6280	1080	220	478	64.3	24.5	15.0	3.5	6.0	1.1	4.0	27.7
Clayey silt layers (n = 41)													
Min	2.1	505	81	46	156	40.6	4.0	4.0	0.9	0.1	0.3	0.1	1.8
Q_1	6.7	832	231	112	390	49.7	6.8	7.2	1.6	0.1	0.3	0.7	3.9
Median	**8.6**	**1800**	**309**	**166**	**430**	**52.7**	**7.5**	**8.0**	**1.9**	**0.1**	**0.4**	**1.0**	**6.2**
Mean	8.0	2100	403	156	428	52.1	7.9	8.9	2.1	0.5	0.6	1.0	5.5
Q_3	9.5	2840	508	201	506	54.5	8.7	10.5	2.4	0.6	0.6	1.4	7.2
Max	14.4	5190	1460	268	642	61.8	14.7	17.5	4.2	1.8	1.2	2.1	9.7

Note: Q_1 = 25th percentile; median = 50th percentile; Q_3 = 75th percentile.

Grain size analysis of the "**sand layers**" (11 samples analyzed) revealed mean grain sizes between 192 and 703 µm, with an average distribution of 88% sand, 9% silt, 2% clay, and sometimes a few granules. All layers with <12% silt are classified as sand. This classification was carried out according to the American Society for Testing and Materials standard ASTM D 2487 [56]. The sandy layers in general have a light brownish color. They are characterized by higher quartz and carbonate contents compared to the silty sand and clayey silt. This is reflected in the significantly higher SiO_2 contents and slightly higher CaO and MgO contents.

The sand layers differ from the other layers by slightly lower metal contents with median metal concentrations of 4.2 wt % Pb, 855 ppm Zn, 248 ppm Sb, 162 ppm Cu, und 106 ppm Ag (Table 3). However, in Figure 6 it can be seen that there are also sandy layers with very high Zn and Cu contents.

With mean grain sizes between 104 and 438 µm, the "**silty sand layers**" consist mainly of fine and very fine sand with more than 12% silt (14 samples analyzed). The average grain size distribution is 70% sand, 27% silt, and 3% clay. The silty sand layers possess various colors of brownish, brownish red, as well as gray hues.

Whereas quartz is enriched in the sand layers, barite (gangue minerals in the mined veins) and muscovite are concentrated in the finer residues. Therefore, SiO_2 contents are lower and BaO, Al_2O_3, and K_2O contents are higher in the silty sand layers compared to the sand layers.

The Ca and Mg concentrations of the various layers decrease with decreasing grain size, which can be attributed to lower amounts of carbonates. Presumably, these lower amounts of carbonates in the silty sand and clayey silt cannot only be traced back to ore sorting processes, but also to the more intense alteration of fine carbonate particles by sulfidic acids in the fine-grained layers due to larger reactive surfaces.

With 5.0 wt % Pb, 1340 ppm Zn, 331 ppm Cu, 306 ppm Sb, and 125 ppm Ag, the metal contents are elevated in the silty sand compared to most of the sand layers (Table 3).

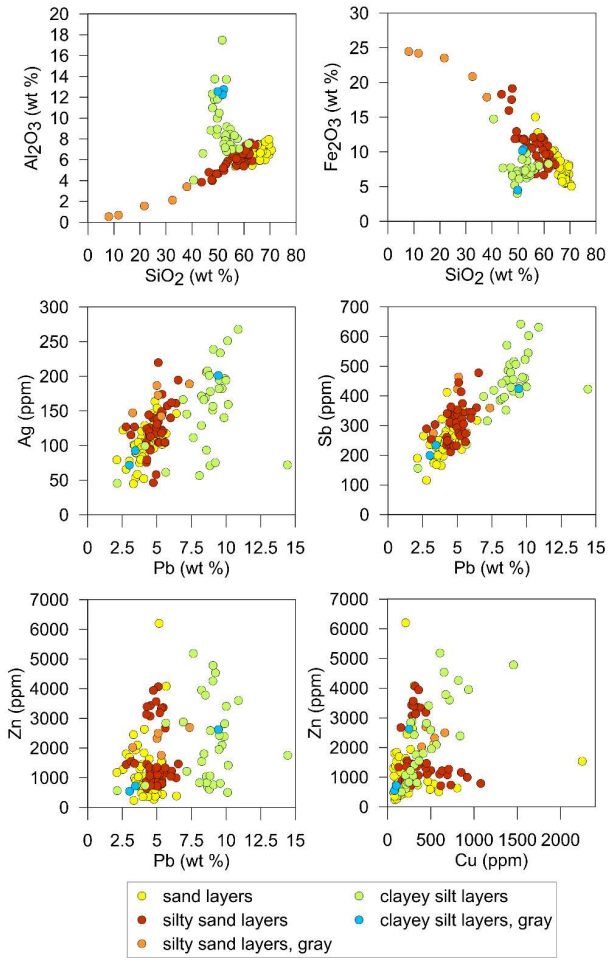

Figure 6. Scatter plots of selected elements for the tailings of the Bergwerkswohlfahrt mine waste dump. Data are based on bulk chemical analyses.

A special feature is silty sand layers of gray color, each up to 10 cm thick, occurring only in one drill core (K). They have a different mineralogical, and hence, a different chemical composition (Figure 6). The very high concentrations of BaO (13–28 wt %) and Fe_2O_3 (18–25 wt %) are accompanied by relatively low SiO_2 values of 8–38 wt % (Figure 6) and are induced by high barite, as well as siderite and partially Fe oxyhydroxide contents, alongside low amounts of quartz. The metal contents of these four layers are in similar concentration ranges as the remaining silty sand layers.

The mean grain sizes of the "**clayey silt layers**" vary between 18 and 30 µm (4 samples analyzed). These finest residues contain 76% silt, 19% clay, and 5% sand on average. The colors vary from ochre to brownish red to gray hues. The clayey silt layers of gray color do not differ in chemical composition from the other layers but show less weathering, and therefore, higher contents of galena, sphalerite, pyrite, and chalcopyrite.

The silty sand and clayey silt layers cannot be differentiated by their SiO_2 content, but rather by the higher Al_2O_3 and K_2O concentrations and lower Fe_2O_3 concentrations in clayey silt layers (Figure 6). Although the median metal concentrations of Pb (8.6 wt %), Zn (1800 ppm), Sb (430 ppm), and Ag (166 ppm) are highest, and Cu concentrations (309 ppm) are high in the clayey silt layers, different distribution patterns can be observed (Table 3), whereas the metal concentrations of Pb, Sb, and partially of Ag increase from coarse-grained sand to fine-grained clayey silt layers; elevated concentrations of Zn and Cu can be found in all types of layers (Figure 6). These differences might be explained by the better cleavage of galena compared to sphalerite and chalcopyrite. Galena is the main host mineral for the majority of Pb, Ag, and Sb. It disintegrates easily upon crushing and was not

recovered during historic processing due to its fine grain size. Another reason for the different metal enrichments is the strong variation of zinc and copper contents in the crude ore.

Among the minor metals, Ga is also enriched (on average 12 ppm in sand, and 16 ppm in clayey silt), especially compared to In and Ge, but these concentrations nevertheless are much too low to warrant thoughts of potential recovery. The same holds true for other minor metals, such as Sn, Mo, W, Bi, and Se, which are generally below 5 ppm for Mo, Se, and In, and below 70 ppm for W and Sn. Therefore, all of these minor metals were not investigated further in this study. Median Cd concentrations are very low (8 ppm Cd, max 46 ppm, n = 88) and As concentrations are slightly elevated (126 ppm As, max 274 ppm, n = 88) within the tailings.

The genesis of the different residue types, namely sand, silty sand, and clayey silt, is probably related to the different steps of the former beneficiation processes. Although in modern tailings from froth flotation there is also an intense layering of clayey, silty, and sandy materials, the observed layering primarily arises from fluvial transport mechanisms, including hydraulic sorting. In this case, the main processes include graded bedding due to grain size and weight differences during disposal of the tailings slurry (if not thickened) and subsequent re-deposition during rainfall events [11,51,57,58]. Such relevant fractionation processes cannot have been of importance during the batch-wise stockpiling of the Bergwerkswohlfahrt mine waste dump.

In general, sand and silty sand layers resemble each other with respect to their bulk chemical composition, as they do not differ too much in their grain size distribution and mineralogical composition. They also show a similar correlation between major elements (e.g., SiO_2, Al_2O_3, Fe_2O_3, K_2O) and valuable metals (Pb, Zn, Ag, Cu, Sb; Figure 6). Obviously, sand and silty sand layers stem from similar or consecutive beneficiation processes, and originate from the same parental material. However, both layer types form distinct units that are clearly distinguishable with the naked eye., which is the reason why they were separated into two different types.

In contrast, the clayey silt exhibits different chemical signatures that are based on a greater variability of the concentrations of Al_2O_3, K_2O, Pb, Sb, Ag, and Zn, and consequently on a lower correlation of various elements between each another. The clayey silt could represent former slurries from the tabling process, which were deposited in basins and heaped up on the dump from time to time. Especially, the approximately 1 m thick layer of this material, apparently covering the northwestern and parts of the central area of the mine waste dump, might have been deposited later. Original small basins with equivalent fine-grained tailings with similar composition were found by the authors at a distance of about 1 km to the studied mine waste dump. However, very thin layers of clayey silt, randomly observed in the drill cores, also could have originated from simple washout and re-deposition of very fine materials, e.g., in puddles.

Implications for recovery: Although the highest average metal contents occur in the clayey silt layers, the other residue types also have high metal concentrations. Selective recovery according to the type of residue is, therefore, not necessary. In addition, a selective recovery would hardly be possible because many layers have only small widths and partially merge into each other. Furthermore, the results of weathering in combination with the metal enrichment in fine layers would complicate potential reprocessing. Lead, for example, is bound to cerussite, galena, as well as metal(loid)-rich Fe oxyhydroxides. These results compare very well to Moles et al. [15] and Pascaud et al. [17], who also name cerussite, anglesite, beudantite and Fe oxyhydroxides as major lead-bearing minerals in their historic tailings from gravity separation.

3.3. Spatial Distribution of the Valuable Elements

Figure 7 shows the observed variations in metal concentration for each drilling core. It is obvious that the maximum Pb and Zn concentrations occur in the northwestern part of the mine waste dump (core A and B). These high concentrations coincide with a high variance. In addition to the maximum Zn values, core A and B also show the highest median Zn grades (2640 ppm and 1630 ppm). For Pb,

the median concentration of drill core L (6.0 wt %) in the central part of the dump is still higher than in core A and B.

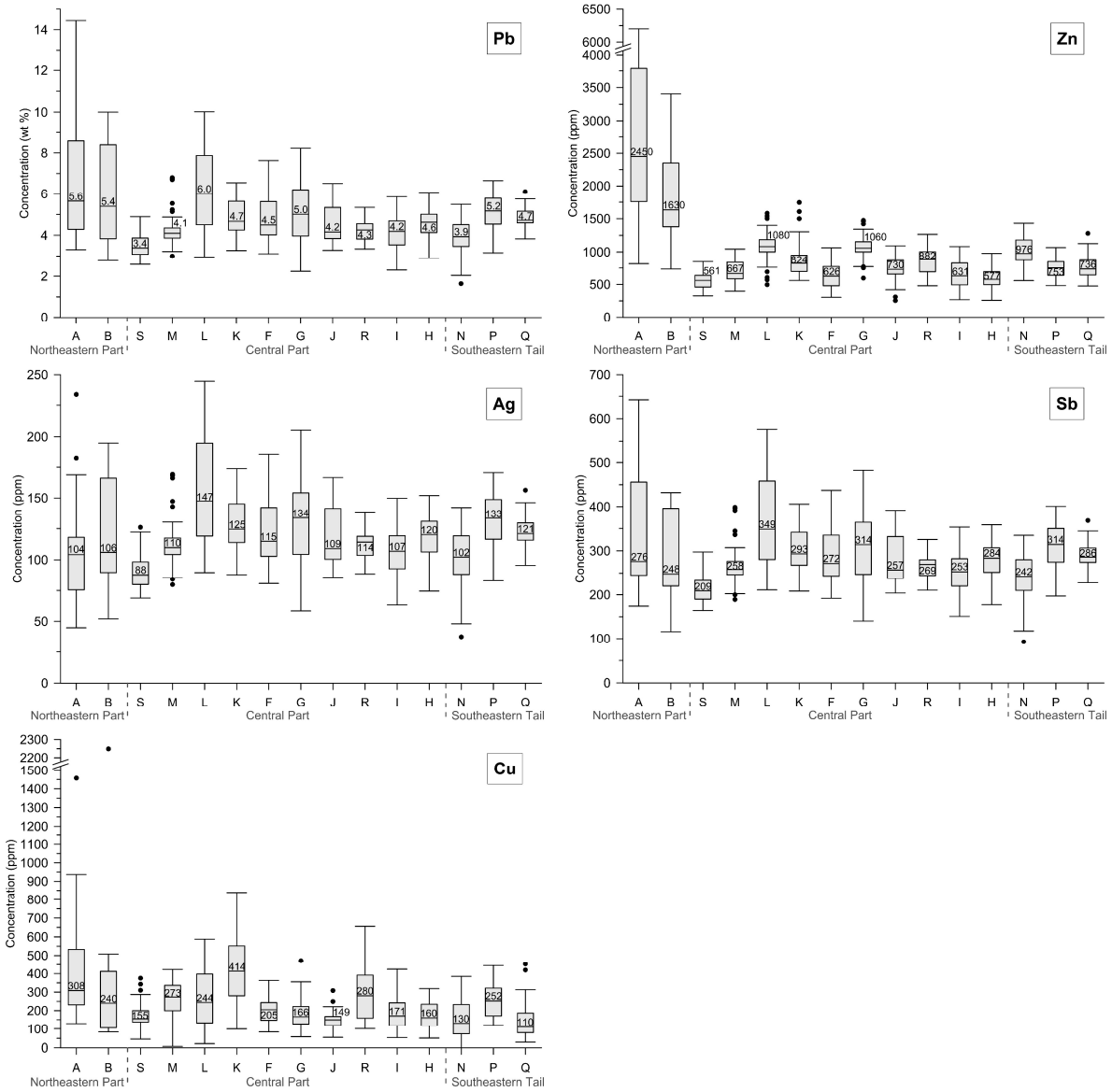

Figure 7. Distribution of the concentrations of Pb, Zn Ag, Sb, and Cu in cores of the Bergwerkswohlfahrt mine waste dump based on bulk chemical analyses (cores A, B, and C) and LIBS analyses (all other cores). The box-and-whisker plots show the median concentration, the 25th and 75th percentiles (quartiles), the whiskers (maximum 1.5 times the interquartile range), as well as possible outliers of each drill core.

Average concentrations of Ag, Sb, and Cu are also elevated in the northwestern part of the mine waste dump, but are even higher in its central part, whereas the highest averaged Ag and Sb concentrations can be found in core L (147 ppm Ag and 349 ppm Sb), while core K has the highest average Cu concentrations (414 ppm Cu).

To get an insight into the spatial distribution of the metals, both with depth and lateral extension, logs of all cores were generated and connected to cross-sections. The longest one is a NW–SE cross-section based on seven logs (Figure 8).

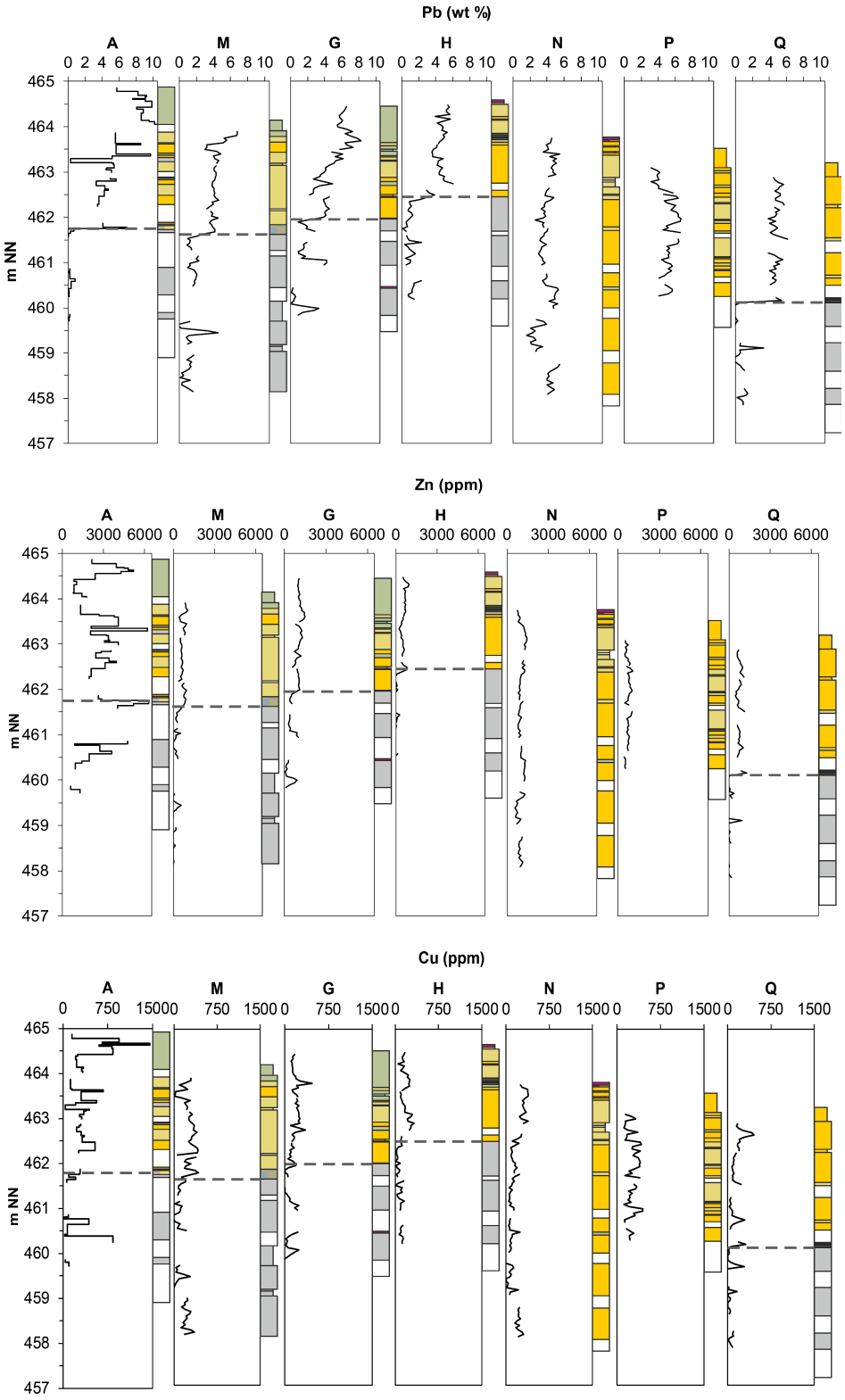

Figure 8. Down-core element profiles along the NW–SE cross-section (cores A–Q). Since Ag and Sb directly correlate with Pb, profiles of these two elements are not shown. For the location of the cross-section see Figure 2, and for lithology see Figure 5.

Concentration profiles of Pb, Ag, and Sb show similar behavior. The majority of Ag and Sb was originally bound to galena. This indicates that despite weathering, the three metals are not very mobile and tend to be bound in, or adsorbed to, nearby weathering products, such as cerussite (Pb, rarely

traces of Ag), Fe oxyhydroxide (Pb, Sb, sometimes Ag), or more rarely, secondary Ag phases (Ag). In the literature a low mobility for Pb and Ag, and a slightly higher mobility for Sb are described at oxidizing and near-neutral conditions with abundant iron-rich particulates [52,59,60].

The comparison of the logs shows a similar pattern in the northwestern to central areas of the mine waste dump with elevated Pb, Ag, and Sb grades in the upper part and decreasing concentrations with depth (drill cores A, B, M, L, F, G, J). In these areas of the mine waste dump metal-enriched layers of clayey silt and partly silty sand occur near the surface.

In drill cores without fine-grained layers or in cores where these layers occur only in deeper parts (drill cores I, H, K, N, P, Q, R, S), a different pattern with relatively constant or slightly increasing Pb, Ag, and Sb concentrations with depth becomes apparent. These drill cores are typical for the central to southwestern area of the mine waste dump (Figure 8). As the drill cores R and S were taken at the slope of the mine waste dump, their concentration profiles might not reflect the original deposition, but may represent the slipped material instead. In drill core O only few tailing materials were encountered, but rocky mine waste was encountered.

The distribution of Zn follows different principles than of Pb, Ag, and Sb, especially in the northwestern area of the mine waste dump, where Zn is extremely enriched. High Zn concentrations cannot be traced back to one specific layer but can be found in all tailing layers. The clayey silt layer in drill core A containing the highest Zn concentration also contains very high Cu concentrations with about 1460 ppm. Although Zn and Cu are in good correlation in many layers of drill core A, in most other drill cores this is not the case. In contrast to Zn, Cu is also found in higher concentrations (between 500 and 840 ppm) in layers of the central area of the mine waste dump (cores K, L, and R). As with Zn, a direct correlation between Cu concentration and layer type is not possible. Hence, the distribution of Zn and Cu in the drill cores to a large extent originates from the inhomogeneity of the original crude ore.

In addition, transport of dissolved zinc and copper may have resulted in a redistribution of both elements [59]. As smithsonite was only found in accessory amounts, the co-precipitation or adsorption of Zn in Fe oxyhydroxides seem to be the dominant solid-phase control for the mobility of Zn, as it is also described for other tailings [61]. In contrast, Cu may have co-precipitated or adsorbed to abundant iron-rich particulates [59].

The results of the mineralogical investigation have shown that the proportions of sulfides and most secondary minerals do not notably change with depth. Only the amount of gypsum increases with depth. Rather, the modal mineralogy seems to be dependent on the grain size distribution and, thus, on the layer type, as well as on the inhomogeneities in the crude ore.

Furthermore, the degree of weathering of the sulfides and carbonates does not significantly decrease with depth. Thus, most of the mine waste dump can be described as a vadose zone, dominated by near-neutral and oxidizing conditions.

Reducing conditions were only observed in a 10–30 cm thick layer in the central area of the mine waste dump. This grey, fine-grained layer of mixed silty sand and clayey silt was observed at the bottom of the cores K, R, and I at 4–6 m depth. There all sulfides were nearly unweathered. This could be explained by rainwater being retained by these fine-grained layers, causing a reducing environment. However, a larger, distinct reduction zone, as often occurs in partially water-saturated tailing impoundments from flotation [11,47], does not exist. With the exception of some very thin coatings of Fe oxyhydroxides around silicates in some near-surface areas and the beginning of cementation by calcite in a few samples from greater depths, no (semi-)indurated layers, such as hardpans or cemented layers [58,61,62], were observed. In addition, efflorescences on the surface of the mine waste dump were not observed during several sampling periods, even in dry periods.

A three-dimensional correlation of specific layers between various cores is not possible. Even in adjacent dill cores (e.g., as they are available in the central area of the waste mine dump) three-dimensional correlations of layers can only be hypothesized but not proven. Most often

only the elevated metal concentrations in the thick layers of clayey silt and some layers of silty sand at the surface of the mine waste dump are discernible.

Obviously, the anthropogenic deposition of the tailings resulted in small-scaled geochemical patterns with no larger patterns, and hence, no geological bedding was derivable. In order to determine the areal relationship of the metal distribution in the mine waste dump, areal variograms were calculated for each metal (Figure 9). Therefore, all drill cores of the central part of the mine waste dump were included, as in this area a high number of closely spaced drill locations occur. The distance of the ten drill cores in the central part varies between 4.5 and 39 m, with half of them only being 6 m apart. The average distance between the ten drill locations (average nearest neighbor) is 8.3 m.

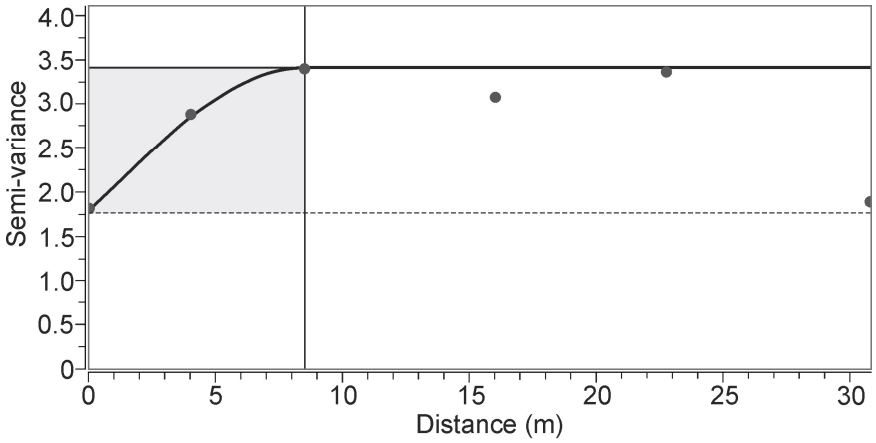

Figure 9. Areal variogram with spherical model (solid line) of all Pb concentrations within ten drill hole locations in the central part of Bergwerkswohlfahrt mine waste dump. Input parameters used for the omnidirectional variogram: lag distance = 8.3 m; number of lags = 5; number of strata = 4. From the variogram a range of 8.6 m, a nugget effect of 1.75, and a sill of 3.4 can be determined.

The computation of the variograms with a spherical model [63,64] was carried out using the software package SKUA-GOCAD® (Subsurface Knowledge Unified Approach - Geological Objects Computer Aided Design; Emerson Paradigm Holding LLC, Houston, TX, USA). For lag distance, the average nearest neighbor at 8.3 m was used and the number of legs was set to five. Depending on the number of strata used, for each element the range of the variogram varies between 7 and 10 m (Figure 9). This means that the metal concentrations of the different drill holes are statistically dependent only within a spatial distance of less than 7–10 m. If drill holes lie further apart, no statement can be made about the spatial relationship of their Pb content, as these data are no longer correlated. These values are consistent with the assumed batch-wise deposition of the different residues at this historic anthropogenic mine waste dump.

Conversely, a geostatistical evaluation of metal concentrations in the mine waste dump, e.g., as part of 3D modeling, is only possible with a maximum drilling grid of 7–10 m. With the exception of a few drill hole locations in the central part, this is by no means the case. Therefore, the metal resources of the Bergwerkswohlfahrt mine waste dump were estimated by descriptive statistics. We assume that the drill cores, which cover all main areas of the dump and their entire longitudinal extent, are representative for the dump. However, it cannot be ruled out that occasionally deviant materials might occur in minor quantities in some areas.

In general, sampling of this type of secondary deposit sufficient for geostatistical modeling would require an enormous amount of drilling and corresponding analytical work. Using a LIBS core scanner can help to reduce the analytical costs, as with a suitable PLS calibration model numerous cores can be analyzed with high resolution and minimal costs. However, the extensive set of material-specific calibration standards that is required for multivariate calibration of the raw LIBS data and the complexities of processing and modeling the data must not be disregarded.

3.4. Resource Estimate

The estimate of the resources of the mine waste dump are based on the data presented in the previous sections. Average metal concentrations in total were extrapolated from the median metal concentrations in the various cores. For the cores F–S, these data are based on the calibrated LIBS data of the 50 mm core intervals (852 total). The profiles for cores A, B, and C, which are based on bulk chemistry measurements, were also used for the resource calculation (64 total). Therefore, each sample from the same drill core was weighed according to its length. For all drill cores only those intervals that were free of rocky or caved materials were used for computation. Hence, data of core O were neglected, as this core only contains small amounts of residues, which, additionally, are partially mixed with rocky material.

The reserve estimate cannot be based on the three different types of residues, as they cannot be mined separately and very often grade into one another. Instead, a regional approach with the three regions, namely the northwestern part, central part, and southwestern tail, was chosen by using the median metal concentration of all weighed samples that belong to the drill cores of the same dump region.

Results of that estimation show distinctively higher Pb (5.4 wt %), Zn (1740 ppm), and Cu (about 240 ppm) concentrations in the northwestern part of the dump compared to the central part and the southern tail (Table 4). For Ag (about 110 ppm) and Sb (about 270 ppm) all regions are characterized by similar concentrations.

Table 4. Average metal concentrations (Pb, Zn, Cu, Ag, and Sb) in the three areas and the total Bergwerkswohlfahrt mine waste dump.

Statistics	Pb wt %	Zn ppm	Cu ppm	Ag ppm	Sb ppm
Total mine waste dump					
Min	1.6	255	0	37	93
Q_1	3.9	778	131	96	232
Median	**4.6**	**973**	**199**	**112**	**269**
Mean	4.9	1100	245	116	285
Q_3	5.7	1310	294	133	333
Max	14.4	7080	2250	245	646
Northwestern part (cores A, B, C, *n* = 64)					
Min	2.3	735	83	45	116
Q_1	4.1	1330	171	80	214
Median	**5.4**	**1740**	**244**	**105**	**267**
Mean	6.3	2230	349	111	319
Q_3	8.6	2670	326	140	432
Max	14.4	7080	2250	234	646
Central part (cores F, G, H, I, J, K, R, S, *n* = 655)					
Min	2.2	255	7	58	140
Q_1	3.8	582	139	100	236
Median	**4.3**	**732**	**200**	**113**	**266**
Mean	4.6	767	240	118	279
Q_3	5.0	946	303	131	308
Max	10.0	1750	838	245	576
Southern tail (cores N, O, P, Q, *n* = 197)					
Min	1.6	477	0	37	93
Q_1	3.9	733	92	100	236
Median	**4.5**	**865**	**168**	**116**	**276**
Mean	4.5	887	183	115	272
Q_3	5.0	1010	258	131	310
Max	6.6	1430	453	171	401

Note: Q_1 = 25th percentile; median = 50th percentile; Q_3 = 75th percentile.

For estimation of the metal concentrations of the mine waste dump in total, the concentrations of the northwestern part were taken as 20%, for the central part as 50%, and for the southern tail as 30%, i.e., more or less proportionally to their respective surface area.

Thus, the average metal concentrations of the Bergwerkswohlfahrt mine waste dump are about 4.6 wt % Pb, 970 ppm Zn, 110 ppm Ag, 200 ppm Cu, and 270 ppm Sb (Table 4).

The volume of the Bergwerkswohlfahrt mine waste dump (excluding the blocky material) is about 82,000 m^3 ± 20%, calculated as one of the results of the geophysical campaign [30]. For a potential deposit this volume is rather small. For the calculation of the tonnage of the Bergwerkswohlfahrt mine waste dump a bulk density of 2.0 t/m^3 was assumed. This bulk density equals the average bulk density of tailings, as given by Bhanbhro [65], Bjelkevik and Knutsson [66], and Büttner et al. [10].

Thus, in total the Bergwerkswohlfahrt mine waste dump is estimated to contain about 8000 t Pb, 180 t Zn, 50 t Sb, 40 t Cu, and 19 t (610,000 ounces) Ag (Table 5).

Table 5. Tonnages and values of metals contained in the Bergwerkswohlfahrt mine waste dump. Parameters used for estimation: volume: 82,000 m^3; bulk density: 2.0 t/m^3.

Economic Parameters	Pb	Zn	Ag	Cu	Sb
Tonnage (t)	8000	180	19	40	50
Average Price 20.18[1] (US$/t; US$/ounce*)	2243	2924	15.71*	6624	8316
Theoretical value (US$), approximately	17,900,000	530,000	9,600,000	260,000	390,000

[1] Source: Federal Institute for Geosciences and Natural Resources (BGR) data bank.

Using the 2018 average metal prices listed in Table 5, the mine waste dump possesses a theoretical value of $28.6 million USD. Of this value, 96% relates to Pb and Ag, with these being the only metals of real commercial interest, at least in this historic mine waste dump. The concentrations of Zn, Cu, and Sb are too low, and therefore, the related tonnages are too small to be of economic interest.

Both tonnages and values refer to the theoretical metal resources, which have to be reduced by the recovery factor. The distribution of valuable metals within the minerals and their state of weathering are crucial for this. Large proportions of the lead bearing mineral galena have been weathered to cerussite and recovery of this lead carbonate is challenging. Dressing tests at the Clausthal University of Technology proved necessary for multi-stage processing, such as leaching–precipitation–flotation (L–P–F) method, which, however, is difficult, and thus, expensive [51]. The lab tests in Clausthal-Zellerfeld produced a lead sulfate concentrate and demonstrated a potential recovery factor of 70% for Pb and 45% for Ag [54]. Thus, the more realistic values of the economic metals Pb and Ag are closer to $12,500,000 USD, and $4,300,000 USD, respectively.

3.5. Economic Potential of Historic Tailings from Gravity Separation

The investigated historic mine waste dump has high economic potential, which seems to be typical for these kinds of old tailings. Obtained metal grades bear similarities with literature data cited in the introduction, i.e., grades of 1–10 wt % Pb, 100 ppm Ag, 60–190 ppm Sb, and 0.9 wt % Cu found in other old tailings [12,15–17,19,67].

However, these literature data should be interpreted with some caution, as obviously some of the other old tailings were only sampled at their surfaces, with few samples analyzed. If sampling of the Bergwerkswohlfahrt mine waste dump was restricted to its surface this would have shown strongly elevated metal concentrations of up to 10 wt % Pb for large areas of fine-grained residues. This is double the value that was obtained by drilling and intense sampling.

Besides possible conflicting uses and other environmental restrictions, there are two main hurdles in recycling historic tailings.

First, a historic tailings site has to be found, where one, or preferentially even more dumps or ponds, are big enough to warrant extraction. This might prove difficult, as the most common method of tailing deposition in early times was the discharge of them into rivers and streams [68]. For example,

in the Harz Mountains, which is an historically important German mining district, the deposition of ore processing residues into streams and rivers lasted at least until the middle or even the end of the 19th century [24,69]. Only due to environmental pressure by farmers did this practice gradually change, with dewatered tailings being dumped on land between the end of the 19th century and the introduction of froth flotation (about 1930). Parts of these dumped tailings were later used as aggregates for construction work. In a radius of 1–10 km from Bergwerkswohlfahrt mine waste dump, there are 3–4 other sites containing old tailings from gravity separation. In general, they are smaller in size than the investigated mine waste dump. In the area of Sierra Mineral of Cartagena-La Unión, Spain, up to 89 tailing dumps are said to exist, which do not stem from froth flotation [18].

It is not possible to calculate worldwide resources for historic tailings from gravity separation as there are hardly any literature data. Two available volumes are 64,100 m^3 for the mine waste dump in Pontigbaud, France [17], and about 100,000 m^3 for the mine waste dump in Albertsgrube, Germany [67]. These volumes are in the same range as the Bergwerkswohlfahrt mine waste dump, and prove that there are limited resources in general.

The second hurdle is the strong weathering of sulfides in the residues—at least in humid climate—as well as the correlation of higher metal concentrations with finer grain sizes.

Based on currently available data, historic tailings most often were piled up in dumps. These dumps are not water-saturated, causing strong weathering of the sulfides. Depending on the prevailing pH-Eh regime, the metals can be mobilized and leached, or fixed in different mineral phases. In the case of Pb this may be cerussite ($PbCO_3$), anglesite ($PbSO_4$), beudantite ($PbFe_3(AsO_4)(SO_4)(OH)_6$), or metal(loid)-rich Fe oxyhydroxides [15,17]. The weathering of the primary sulfides, and therefore, the distribution of the metals in sulfides, carbonates, or oxyhydroxides, as well as the enrichment of some metals in finer grain sizes, may restrict reprocessing and make more efficient reprocessing methods necessary.

However, the limited volume of only up to 100,000 m^3 of these historic tailings will not warrant new and separate treatment plants. With mobile or modular ore processing plants, this hurdle can be overcome. Mobile plants can also be used to reprocess tailings of interest in larger mining districts. Whereas the metal content of these historic tailings may be limited and treatment may be difficult, recycling might finance the remediation costs, if required.

4. Conclusions

Historic tailings from gravity separation very often contain elevated metal concentrations, which in general are much higher than concentrations in modern flotation tailings. This is based on the straightforward ore processing steps of crushing, classification, and sorting by gravity in former times. Historic tailings of interest are mainly restricted to mining districts that were active between 1850 and 1930.

The studied mine waste dump, being representative for historic tailings, proved to be very heterogeneous, as is recognizable by the strong alternation of sand, silty sand, and clayey silt layers. As a result of the deposition of the residues in rather small and separate batches, the geochemical and mineralogical composition, and therefore the metal grades, vary strongly within short distances. Drilling, therefore, is highly recommended for future exploration of these type of deposits. The application of a LIBS core scanner is very convenient for detailed spatial analysis of a large number of drill cores, as it can help to reduce exploration costs, as more cores can be analyzed within a shorter time period. However, a disadvantage is the extensive set of material-specific calibration standards that are required for multivariate LIBS calibration.

A selective recycling of individual grain size classes is not necessary, as high metal concentrations occur in all grain size fractions. Valuable metals not only occur in the primary sulfides, but also in secondary phases, especially cerussite and Fe oxyhydroxides. Based on the strong weathering of the sulfides under the prevailing oxidizing conditions, as well as the high content of very fine grain sizes, efficient tailor-made reprocessing methods are necessary.

In the mine waste dump under investigation, only Pb and Ag are of economic interest. With a total tonnage close to 8000 t of lead and 610,000 ounces of silver, the Bergwerkswohlfahrt mine waste dump can be classified as an interesting but limited secondary resource. Although of limited economic value, recycling might finance future remediation costs.

A literature review has shown that historic mine dumps are typically limited in volume to a maximum of 100,000 m^3. However, they may occur in nearby clusters. Therefore, mobile and modular ore processing plants could be a solution for recovering valuable materials from different tailing sites within a mining district.

Author Contributions: Conceptualization, K.K.; methodology, K.K. and J.M.; formal analysis and investigation, K.K. and J.M.; writing—original draft preparation, K.K.; writing—review and editing, K.K. and J.M.

Funding: This research was part of the ROBEHA research project ("Nutzung des Rohstoffpotenzials von Bergbau- und Hüttenhalden unter Berücksichtigung der Nachhaltigkeit am Beispiel des Westharzes"), funded by the German Federal Ministry of Education and Research (BMBF), FKZ: 033R105F.

Acknowledgments: We gratefully thank our colleagues at BGR: D. Rammlmair and H. Elsner for fruitful discussions, F. Korte and E. Gäbler for the bulk chemical analyses, as well as D. Göricke and M. Brockmann for the support in drilling. We also would like to thank our project partners T. Martin, R. Kniess, and U. Noell from BGR, as well as E. Gock, H. Saheli, and Z. Ma from the Clausthal University of Technology for collaboration and fruitful discussions. Special thanks go to Mr. Witte for allowing access to his property.

Conflicts of Interest: The authors declare no conflict of interest.

References

1. Hudson-Edwards, K.A.; Jamieson, H.E.; Lottermoser, B.G. Mine Wastes: Past, Present, Future. *Elements* **2011**, *7*, 375–380. [CrossRef]
2. Jambor, J.L.; Blowes, D.W.; Ritchie, A. Environmental Aspects of Mine Wastes. *Proc. Miner. Assoc. Can. Short Course Ser.* **2003**, *31*, 430.
3. Jacobs, J.A.; Lehr, J.H.; Testa, S.M. *Acid Mine Drainage, Rock Drainage, and Acid Sulfate Soils: Causes, Assessment, Prediction, Prevention, and Remediation*; John Wiley & Sons, Inc.: Hoboken, NJ, USA, 2014; p. 504.
4. Lottermoser, B.G. *Mine Wastes: Characterization, Treatment and Environmental Impacts*, 3rd ed.; Springer: Berlin/Heidelberg, Germany, 2003; p. 400.
5. Dold, B. Evolution of Acid Mine Drainage Formation in Sulphidic Mine Tailings. *Minerals* **2014**, *4*, 621–641. [CrossRef]
6. Dold, B. Submarine tailings disposal (STD)—A review. *Minerals* **2014**, *4*, 642–666. [CrossRef]
7. Leblanc, M.; Morales, J.A.; Borrego, J.; Elbaz-Poulichet, F. 4500-year-old mining pollution in southwestern Spain: Long-term implications for modern mining pollution. *Econ. Geol.* **2000**, *95*, 655–662. [CrossRef]
8. Thomassen, B. The Blyklippen lead-zinc mine at Mesters Vig, East Greenland. *Geol. Ore* **2005**, *5*, 12.
9. Woltemate, I. Beurteilung der Geochemischen und Sedimentpetrographischen Aussagefähigkeit von Bohrproben aus Flotationsabgängen in Zwei Absitzbecken des Erzbergwerks Rammelsberg. Ph.D. Thesis, Clausthal University of Technology, Clausthal-Zellerfeld, Germany, 1988.
10. Büttner, P.; Osbahr, I.; Zimmermann, R.; Leißner, T.; Satge, L.; Gutzmer, J. Recovery potential of flotation tailings assessed by spatial modelling of automated mineralogy data. *Miner. Eng.* **2018**, *116*, 143–151. [CrossRef]
11. Holmström, H.; Salmon, U.J.; Carlsson, E.; Petrov, P.; Öhlander, B. Geochemical investigations of sulfide-bearing tailings at Kristineberg, northern Sweden, a few years after remediation. *Sci. Total Environ.* **2001**, *273*, 111–133. [CrossRef]
12. Gordon, R.B. Production residues in copper technological cycles. *Resour. Conserv. Recycl.* **2002**, *36*, 87–106. [CrossRef]
13. Morin, D.H.R.; d'Hugues, P. Bioleaching of a Cobalt-Containing Pyrite in Stirred Reactors: A Case Study from Laboratory Scale to Industrial Application. In *Biomining*; Rawlings, D.E., Johnson, D.B., Eds.; Springer: Berlin/Heidelberg, Germany, 2007; pp. 35–55.
14. Moss, R.; Poblete de la Cerda, R. *Technical Review of Operations at Minera Valle Central Rancagua Region VI, Chile*; Amerigo Resource LTD: Vancouver, BC, Canada, 2006; p. 94.

15. Moles, N.R.; Smyth, D.; Maher, C.E.; Beattie, E.H.; Kelly, M. Dispersion of cerussite-rich tailings and plant uptake of heavy metals at historical lead mines near Newtownards, Northern Ireland. *Appl. Earth Sci.* **2004**, *113*, 21–30. [CrossRef]
16. Bellenfant, G.; Guezennec, A.-G.; Bodénan, F.; D'Hugues, P.; Cassard, D. Re-processing of mining waste: Combining environmental management and metal recovery? In Proceedings of the Mine Closure 2013, Eden, UK, 14–22 September 2013; pp. 571–582.
17. Pascaud, G.; Lévèque, T.; Soubrand, M.; Boussen, S.; Joussein, E.; Dumat, C. Environmental and health risk assessment of Pb, Zn, As and Sb in soccer field soils and sediments from mine tailings: Solid speciation and bioaccessibility. *Environ. Sci. Pollut. Res.* **2014**, *21*, 4254–4264. [CrossRef] [PubMed]
18. García-Lorenzo, M.L.; Pérez-Sirvent, C.; Martínez-Sánchez, M.J.; Molina-Ruiz, J. Trace elements contamination in an abandoned mining site in a semiarid zone. *J. Geochem. Explor.* **2012**, *113*, 23–35. [CrossRef]
19. Silver Pursuit Resources Ltd. Newsfile, Marketwire. Available online: https://www.goldseiten.de/artikel/143510--Silver-Pursuit-Resources-Ltd.~{}-Historic-Mine-Dumps-at-La-Quintera-Project-Mexico.html (accessed on 21 October 2011).
20. Khajehzadeh, N.; Haavisto, O.; Koresaar, L. On-stream and quantitative mineral identification of tailing slurries using LIBS technique. *Miner. Eng.* **2016**, *98*, 101–109. [CrossRef]
21. Kuhn, K.; Meima, J.A.; Rammlmair, D.; Ohlendorf, C. Chemical mapping of mine waste drill cores with laser-induced breakdown spectroscopy (LIBS) and energy dispersive X-ray fluorescence (EDXRF) for mineral resource exploration. *J. Geochem. Explor.* **2016**, *161*, 72–84. [CrossRef]
22. Bartels, C. *Das Erzbergwerk Grund*; Preussag AG Metall: Goslar, Germany, 1992; p. 149.
23. Liessmann, W. *Historischer Bergbau im Harz*; Springer: Berlin/Heidelberg, Germany, 2010.
24. Preußische Bergwerks- und Hütten-Aktiengesellschaft. *Akten Bergamt Goslar, W4002/I Betriebspläne 1893–1903*; Bergarchiv Clausthal, Landesamt für Bergbau, Energie und Geologie: Clausthal-Zellerfeld, Germany, 1903.
25. Hawley, M.; Cunning, J. *Guidelines for Mine Waste Dump and Stockpile Design*; CRC Press/Balkema: Leiden, The Netherlands, 2017; p. 385.
26. Weltkarte.com. Topographic Map of Germany. Available online: www.weltkarte.com (accessed on 4 April 2019).
27. Poggendorf, C.; Rüpke, A.; Gock, E.; Saheli, H.; Kuhn, K.; Martin, T. Nutzung des Rohstoffpotentials von Bergbau- und Hüttenhalden am Beispiel des Westharzes. In *Mineralische Nebenprodukte und Abfälle 2—Aschen, Schlacken, Stäube und Baurestmassen*; Thomé-Kozmiensky, K.J., Ed.; TK Verlag: Neuruppin, Germany, 2015; pp. 580–602.
28. Landesamt für Geoinformation und Landesvermessung Niedersachsen (LGLN). *Digital Arial Photos of ATKIS*; LGLN: Hannover, Germany, 2005.
29. Landkreis Goslar—Fachdienst Umwelt. *Altlastenkataster Landkreis Goslar*; Landkreis Goslar: Goslar, Germany, 2011.
30. Martin, T.; Kuhn, K.; Günther, T.; Kniess, R. Geophysical Exploration of a historical stamp mill dump for the estimation of valuable residuals. Manuscript in preparation.
31. Martin, T.; Knieß, R.; Noell, U.; Hupfer, S.; Kuhn, K.; Günther, T. Geophysical exploration of historical mine dumps for the estimation of valuable residuals. In Proceedings of the EGU General Assembly 2015, Vienna, Austria, 12–17 April 2015.
32. Kniess, R.; Martin, T. Reconstruction of the inner structure of small scale mining waste dumps by combining GPR and ERTdata. In Proceedings of the EGU General Assembly 2015, Vienna, Austria, 12–17 April 2015.
33. Body, D.; Chadwick, B.L. Optimization of the spectral data processing in a LIBS simultaneous elemental analysis system. *Spectrochim. Acta Part B Atomic Spectrosc.* **2001**, *56*, 725–736. [CrossRef]
34. Cremers, D.A.; Radziemski, L.J. *Handbook of Laser-Induced Breakdown Spectroscopy*; John Wiley & Sons Ltd.: Chichester, UK, 2006; p. 283.
35. Miziolek, A.W.; Palleschi, V.; Schechter, I. *Laser-Induced Breakdown Spectroscopy (LIBS)*; Cambridge University Press: Cambrdige, MA, USA, 2006; p. 620.
36. Sirven, J.-B.; Bousquet, B.; Canioni, L.; Sarger, L. Laser-Induced Breakdown Spectroscopy of Composite Samples: Comparison of Advanced Chemometrics Methods. *Anal. Chem.* **2006**, *78*, 1462–1469. [CrossRef]
37. Yaroshchyk, P.; Death, D.L.; Spencer, S.J. Comparison of principal components regression, partial least squares regression, multi-block partial least squares regression, and serial partial least squares regression algorithms for the analysis of Fe in iron ore using LIBS. *J. Anal. Atomic Spectrom.* **2012**, *27*, 92–98. [CrossRef]

38. Takahashi, T.; Thornton, B. Quantitative methods for compensation of matrix effects and self-absorption in Laser Induced Breakdown Spectroscopy signals of solids. *Spectrochim. Acta Part B Atomic Spectrosc.* **2017**, *138*, 31–42. [CrossRef]
39. Amador-Hernández, J.; Garcia-Ayuso, L.E.; Fernandez-Romero, J.M.; Luque de Castro, M.D. Partial least squares regression for problem solving in precious metal analysis by laser induced breakdown spectrometry. *J. Anal. Atomic Spectrom.* **2000**, *15*, 587–593. [CrossRef]
40. Wold, S.; Sjöström, M.; Eriksson, L. PLS-regression: A basic tool of chemometrics. *Chemomet. Intell. Lab. Syst.* **2001**, *58*, 109–130. [CrossRef]
41. Geladi, P.; Kowalski, B.R. Partial least-squares regression: A tutorial. *Anal. Chim. Acta* **1986**, *185*, 1–17. [CrossRef]
42. Höskuldsson, A. PLS regression methods. *J. Chemomet.* **1988**, *2*, 211–228. [CrossRef]
43. Naes, T.; Martens, H. Comparison of prediction methods for multicollinear data. *Commun. Stat. Simul. Comput.* **1985**, *14*, 545–576. [CrossRef]
44. Wold, S.; Ruhe, A.; Wold, H.; Dunn, I.W. The Collinearity Problem in Linear Regression. The Partial Least Squares (PLS) Approach to Generalized Inverses. *SIAM J. Sci. Stat. Comput.* **1984**, *5*, 735–743. [CrossRef]
45. Mevik, B.-H.; Wehrens, R.; Liland, K.H.; Hiemstra, P. pls: Partial Least Squares and Principal Component Regression. R Package Version 2.7–0. Available online: https://CRAN.R-project.org/package=pls (accessed on 21 August 2018).
46. Kuhn, K.; Graupner, T.; Langer, A. Hightech-Rohstoffe aus niedersächsischen und anderen deutschen Primär- und Sekundärquellen. *Akademie für Geowissenschaften und Geotechnologien* **2015**, *31*, 45–54. [CrossRef]
47. Jambor, J.L. Mineralogy of sulfide-rich tailings and their oxidation products. In *Short Course Handbook on the Environmental Geochemistry of Sulfide Mine-Wastes*; Jambor, J.L., Blowes, D.W., Eds.; Mineralogical Association of Canada: Waterloo, ON, Canada, 1994; Volume 22, pp. 59–102.
48. Plumlee, G.S. The Environmental Geology of Mineral Deposits. In *The Environmental Geochemistry of Mineral Deposits*; Plumlee, G.S., Logsdon, M.J., Eds.; Society of Economic Geologists: Littleton, CO, USA, 1999; Volume 6A, pp. 71–116.
49. Ptacek, C.J.; Blowes, D.W. Influence of siderite on the pore-water chemistry of inactive mine tailings impoundments. In *Environmental Geochemistry of Sulfide Oxidation*; Alpers, C.N., Blowes, D.W., Eds.; American Chemical Society: Washington, DC, USA, 1994; Volume 550, pp. 172–189.
50. Paktunc, A.D.; Davé, N.K. Formation of secondary pyrite and carbonate minerals in the Lower Williams Lake tailings basin, Elliot Lake, Ontario, Canada. *Am. Miner.* **2002**, *87*, 593–602. [CrossRef]
51. Blowes, D.W.; Ptacek, C.J.; Jurjovec, J. Mill tailings: Hydrogeology and geochemistry. In *Environmental Aspects of Mine Wastes*; Jambor, J.L., Blowes, D.W., Ritchie, A.I.M., Eds.; Mineralogical Association of Canada: Vancouver, BC, USA, 2003; Volume 31, pp. 95–116.
52. Jamieson, H.E.; Walker, S.R.; Parsons, M.B. Mineralogical characterization of mine waste. *Appl. Geochem.* **2015**, *57*, 85–105. [CrossRef]
53. DIN Deutsches Institut für Normung e.V. *DIN 38 414–4: Deutsche Einheitsverfahren zur Wasser-, Abwasser- und Schlammuntersuchung; Schlamm und Sedimente (Gruppe S); Bestimmung der Eluierbarkeit mit Wasser (S 4)*; Beuth: Berlin, Germany, 1984.
54. Gock, E.; Saheli, H.; Ma, Z. *Nutzung des Rohstoffpotenzials von Bergbau- und Hüttenhalden unter Berücksichtigung der Nachhaltigkeit am Beispiel des Westharzes—Final Report of BMBF-Research Project ROBEHA, Sub-Project 4: Aufbereitung (Reprocessing)*; TU Clausthal: Clausthal-Zellerfeld, Germany, 2016; p. 128.
55. Blowes, D.; Ptacek, C. Acid-neutralization mechanisms in inactive mine tailings. In *The Environmental Geochemistry of Sulfide Mine-Wastes*; Jambor, J.L., Blowes, D.W., Eds.; Mineralogical Association of Canada: Waterloo, ON, Canada, 1994; Volume 22, pp. 271–292.
56. American Society for Testing and Materials. *Classification of Soils for Engineering Purposes: Annual Book of ASTM Standards*; D 2487–83; ASTM International: West Conshohocken, PA, USA, 1985; pp. 395–408.
57. Nikonow, W.; Rammlmair, D.; Furche, M. A multidisciplinary approach considering geochemical reorganization and internal structure of tailings impoundments for metal exploration. *Appl. Geochem.* **2019**, *104*, 51–59. [CrossRef]
58. Graupner, T.; Kassahun, A.; Rammlmair, D.; Meima, J.A.; Kock, D.; Furche, M.; Fiege, A.; Schippers, A.; Melcher, F. Formation of sequences of cemented layers and hardpans within sulfide-bearing mine tailings (mine district Freiberg, Germany). *Appl. Geochem.* **2007**, *22*, 2486–2508. [CrossRef]

59. Smith, K.S.; Huyck, H.L.O. An overview of the abundance, relative mobility, bioavailability, and human toxicity of metals. In *The Environmental Geochemistry of Mineral Deposits*; Plumlee, G.S., Logsdon, M.J., Eds.; Society of Economic Geologists: Littleton, CO, USA, 1999; Volume 6A, pp. 29–70.
60. MEND (Mine Environment Neutral Drainage program). *Review of Water Quality Issues in Neutral pH Drainage: Examples and Emerging Priorities for the Mining Industry in Canada*; MEND Initiative: Ottawa, ON, Canada, 2004; p. 58.
61. Moncur, M.C. Release, transport and attenuation of metals from an old tailings impoundment. *Appl. Geochem.* **2005**, *20*, 639–659. [CrossRef]
62. Blowes, D.W. The pore-water geochemistry and the mineralogy of the vadose zone of sulfide tailings, Waite Amulet, Quebec, Canada. *Appl. Geochem.* **1990**, *5*, 327–346. [CrossRef]
63. Bailey, T.C.; Gatrell, A.C. *Interactive Spatial Data Analysis*; Longman Scientific & Technical: Essex, UK, 1995; p. 413.
64. Oliver, M.A.; Webster, R. A tutorial guide to geostatistics: Computing and modelling variograms and kriging. *CATENA* **2014**, *113*, 56–69. [CrossRef]
65. Bhanbhro, R. *Mechanical Properties of Tailings: Basic Description of a Tailings Material from Sweden*; Luleå University of Technology: Luleå, Sweden, 2014.
66. Bjelkevik, A.; Knutsson, S. Swedish tailings-comparison of mechanical properties between tailings and natural geological materials. In Proceedings of the Securing the Future: International Conference on Mining and the Environment Metals and Energy Recovery, Skellefteå, Sweden, 27 June–1 July 2005; p. 117.
67. Hensler, A.-S.; Lottermoser, B.G.; Vossen, P.; Langenberg, L.C. Automated Mineral Analysis to Characterize Metalliferous Mine Waste. *IOP Conf. Series Earth Environ. Sci.* **2016**, *44*, 052046. [CrossRef]
68. Wills, B.A. *Mineral Processing Technology*, 4th ed.; Pergamon Press: New York, NY, USA, 1988.
69. Kornacker, J. Die Schädigung der Landwirtschaft im Innerstetal durch Pochsand. In *Hildesheimsche Zeitung, 214*; Bergarchiv Clausthal, Landesamt für Bergbau, Energie und Geologie: Clausthal-Zellerfeld, Germany, 1907.